INFLUENCE OF MICRO-STRUCTURE ON FIBRE PUSH-OUT TESTS

Barthel Brylka[1)], Felix Fritzen[1)], Thomas Böhlke[1)], Kay André Weidenmann[2)]

[1)] Chair for Continuum Mechanics, Institute of Engineering Mechanics, Department of Mechanical Engineering, Karlsruhe Institute of Technology (KIT), POB 6980, 76128 Karlsruhe, Germany

[2)] Institute of Materials Science and Engineering I (IWK 1), Department of Mechanical Engineering, Karlsruhe Institute of Technology (KIT), POB 6980, 76128 Karlsruhe, Germany

Corresponding author: brylka@itm.uni-karlsruhe.de

1. Introduction

The investigations presented in this paper focus on the simulation of push-out tests on a long fibre reinforced thermoplastic (LFT) manufactured in a compression moulding process. The microstructure of LFT is strongly influenced by the manufacturing process and shows inhomogeneous distribution and orientation of the glass fibres. Figure 1 shows the surface of a polished specimen, which has been cut normal to the melt flow direction.

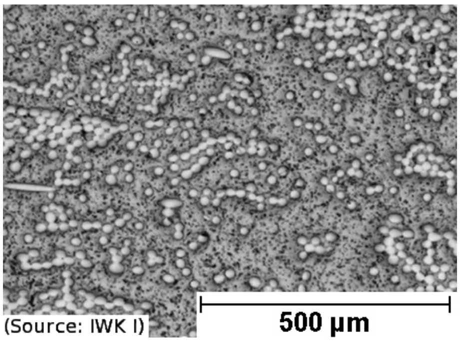

Fig. 1: Surface of polished LFT specimen

The influence of geometrical parameters like, e.g., fibre arrangements and fibre misalignment is still not fully understood. For the interpretation of experimental data the afore-mentioned parameters must be taken into account. Therefore, a numerical study is performed to determine these influences on the mechanical behaviour in push-out experiments.

2. Numerical Methods

For the finite element simulation, a linear-elastic behaviour of glass and polypropylene has been assumed with the additional assumption that the two phases (i.e. the matrix and the fibres) are initially perfectly bonded. To describe the interface model, the separation of the surfaces at the interface $\boldsymbol{\delta}$ will be related by the isotropic effective interface stiffness $\boldsymbol{K}$ due to ongoing damaging process with the traction on the interface $\boldsymbol{t}$ by $\boldsymbol{t} = \boldsymbol{K}\boldsymbol{\delta}$ [1]. This effective stiffness $\boldsymbol{K}$ is related to the initial stiffness $\boldsymbol{K}^0$ by the scalar damage variable D via $\boldsymbol{K} = (1\text{-}D)\boldsymbol{K}^0$. Starting from an undamaged interface $\boldsymbol{K} = \boldsymbol{K}^0$, i.e. $D = 0$, the onset of interface damage is described by the pressure-independent damage initiation criterion $\varphi(\boldsymbol{t}^*)$ ($\langle\bullet\rangle = \max(\bullet,0)$)

$$\varphi(\boldsymbol{t}^*) = \boldsymbol{t}^* \cdot (\boldsymbol{G}\,\boldsymbol{t}^*) \leq 1 \,, \quad \boldsymbol{G} = (\tau_c^{-2})\,\boldsymbol{I} \,,$$

$$\boldsymbol{t}^* = (\boldsymbol{I}\text{-}\boldsymbol{n}\otimes\boldsymbol{n})\boldsymbol{t} + \langle \boldsymbol{t}\cdot\boldsymbol{n}\rangle \boldsymbol{n} \,.$$

Hence, the isotropic second-order damage initiation tensor $\boldsymbol{G}$ depends only on one interface strength τ_c. To describe the evolution of the damage variable D, the effective separation $\delta_e = \| \boldsymbol{\delta} \|$ and its maximal value δ_e^{max} over the time history have been used together with the effective separation at the damage initiation δ_e^0 and the effective separation at the complete interface failure δ_e^f

$$D = \frac{\delta_e^f}{\delta_e^f - \delta_e^0}\left(1 - \frac{\delta_e^0}{\delta_e^{\max}}\right).$$

According to the investigations of Zhandarov et al. [2], the interface strength has been assumed as $\tau_c = 18$ MPa, and the interface fracture energy to $\Gamma = 2{,}96$ J/m². These parameters have been used for all simulations. The fibre diameter is 10 µm, the specimen thickness is h=100 µm. For the simulation of push-out tests, the interface model provided by ABAQUS has been used.

3. Results

Figure 2 shows the shear traction, the damage initiation criterion $\varphi(\boldsymbol{t}^*)$ and the damage variable D on the interface at the maximum force of the indenter, for the reference model with a single and centric embedded fibre which is oriented parallel to the push-out direction.

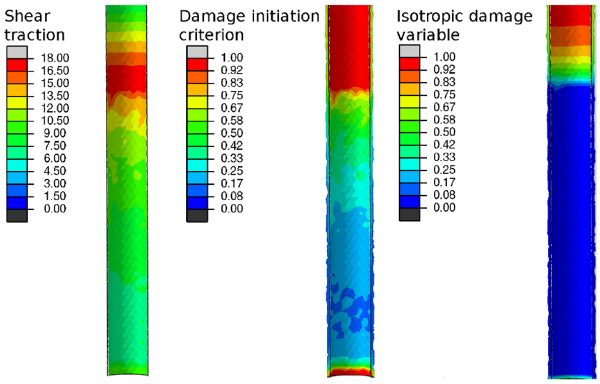

Fig. 2: Plot of the interface field variables for the reference model.

It is apparent that after the onset of interface damage the reaction force on the indenter is still increasing. For this reason, the value of the peak force depends on the damage model, the assumed interface strength τ_c, and the fracture energy Γ. To study the sensitivity of the indentation force peak with respect to varying microstructures, the results from the simulations with modified position or orientation of the single fibre as well as the simulation with interacting fibres are compared to the reference model. All the variations of the topological parameters have been calculated stepwise in defined ranges. The influence of the eccentricity has been calculated in a range of 40 µm in steps of 5 µm, the influence of the inclination angle has been calculated from 0° to 25° in 5° steps, and for the fibre interaction models, the distance between the fibres has been varied in 2 µm steps. Additionally, two multifibre models have been analyzed with random choice of the investigated parameters.

Figure 3 shows for example the computed curves of the indenter force over the displacement for the study on fibre density.

The range of the varied geometrical parameters leads to the band width of the particular peaks of reaction forces given in Figure 4.

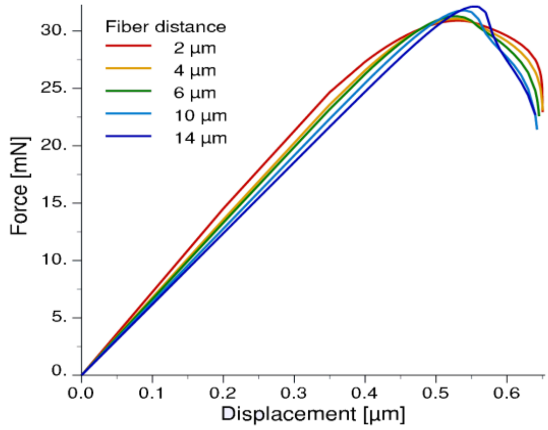

Fig. 3: Computed force-displacement-curves for the study of fibre density.

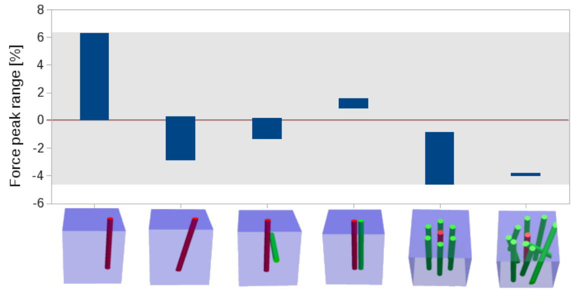

Fig. 4: Comparison of the peak force ranges for the examined cases of fibre topology (left to right) die slot distance, fibre inclination, two fibre models (orthogonal/parallel fibres), fibre clustering, random multifibre models.

4. Conclusion

The results show that the influence of the fibre topology in the specimen on the peak force is found in a range of 10 %.

Mainly the fibre position related to the die slot and the fibre density influence the deviation of the peak force. By comparing the results of the random multifibre models it can be assumed that the experimental results for a real microstructure of a long fibre reinforced thermoplastic should not exceed this range.

References

[1] ABAQUS Analysis User's Manual, Version 6.9, Part IX, Chapter 3, 32.1.10.

[2] Z. Zhandarov, E. Pisanova and E. Mäder, Compos. Sci. Technol. 19, 679-704 (2005).

[3] Z. Zhandarov and E. Mäder, Compos. Sci. Technol. 65, 149-160 (2005).